An Assessment of the Mechanism of Initial Electron Transfer in Bacterial Reaction Centers†

Christine Kirmaier* and Dewey Holten*

Department of Chemistry, Washington University, St. Louis, Missouri 63130

Received October 24, 1990; Revised Manuscript Received November 29, 1990

ABSTRACT: Subpicosecond time-resolved photodichroism measurements on *Rhodobacter sphaeroides* R26 reaction centers are reported in the key region between 620 and 740 nm, where the anions of both bacteriopheophytin and bacteriochlorophyll (BChl) have their most diagnostic absorption bands. These measurements fail to resolve clearly the formation of a reduced BChl species. The implications of this for elucidating the role of the accessory BChl in the initial stage of charge separation are discussed.

The involvement of the monomeric bacteriochlorophyll associated with the L-polypeptide ($BChl_L$) in electron transfer from the bacteriochlorophyll dimer (P) to the L-side bacteriopheophytin (BPh_L) is one of the most controversial issues regarding photochemistry in photosynthetic bacterial reaction centers (RCs). Experimental results (Breton et al., 1988; Holzapfel et al., 1989, 1990; Kirmaier & Holten, 1990; Lockhart et al., 1988, 1990; Wasielewski & Tiede, 1986; Woodbury et al., 1985) and theoretical arguments (Bixon et al., 1989; Friesner & Won, 1989; Hu & Mukamel, 1989; Kitzing & Kuhn, 1990; Scherer & Fischer, 1989; Warshel et al., 1988) favoring both the superexchange and the two-step chemical intermediate mechanisms have been presented in recent years. There is agreement that, for the latter mechanism ($P^* \rightarrow P^+BChl_L^- \rightarrow P^+BPh_L^-$) to hold, $P^+BChl_L^-$ must have a lifetime much shorter than the P^* lifetime of ~3 ps. Recent picosecond studies have indicated that the near-infrared kinetic data are more complex than previously had been thought and appear to require ~1- and ~3-ps components at a minimum to adequately describe the early time course of the absorption changes. Holzapfel et al. (1989, 1990) have interpreted this complexity as evidence for the intermediacy of $P^+BChl_L^-$. However, this conclusion is not straightforward, especially in view of our finding of an analogous 3-fold variation with wavelength of the time constant for the subsequent slower $P^+BPh_L^- \rightarrow P^+Q_A^-$ electron transfer step (Kirmaier & Holten, 1990). We have suggested that the wavelength variation of the apparent time constants for both electron transfer steps arises from a distribution of RCs, with an associated distribution of rates. This complexity makes it difficult to unambiguously assign a 1-ps component to the decay of $P^+BChl_L^-$.

We consider here the 620–740-nm spectral region where the BPh_L anion has a broad absorption band centered near 665 nm and where $BChl_L^-$ should also have an absorption band (Fajer et al., 1975). Picosecond photodichroism measurements on RCs (Kirmaier et al., 1983, 1985, 1989) may be especially valuable in this region since the anion bands of BPh_L and $BChl_L$ are expected to have different polarizations. Recently, Holzapfel et al. (1989, 1990) have interpreted photodichroism data at 665 nm as evidence for formation of $P^+BChl_L^-$. We show here that our data in this region, acquired under essentially the same experimental conditions, are significantly different and examine simulations of the kinetics under the one- and two-step mechanisms for the initial charge separation process.

Experimental Procedures

The apparatus used in this work is based on a mode-locked cw Nd:YAG/synchronously pumped dye laser system equipped with two pulse compressors and a three-stage Q-switched Nd:YAG-pumped dye amplifier (all Spectra Physics), providing ~100-fs ~250-μJ pulses at 582 nm at 10 Hz. Half of this output is used to generate white-light probe flashes and the second half to produce ~15-μJ ~100-fs 870-nm excitation flashes (generated from a second continuum and a two-stage LDS-867 dye amplifier). The 870-nm flashes were focused to ~1.5 mm in diameter at the sample and attenuated as indicated below. The time-resolved photoselection measurements were carried out basically as described previously with HR polarizers (Polaroid) to ensure polarization of the 870-nm flashes and a Glan-Taylor prism to select a polarization of the probe light either parallel or perpendicular to the excitation light (Kirmaier et al., 1983, 1985).

Data were acquired over the entire anion region (620–740 nm) with points at 0.3-nm intervals on a two-dimensional vidicon-based detection system [see Kirmaier et al. (1985, 1989)]. Group velocity dispersion in the probe pulse results in a chirp of ~6 fs/nm across the acquired spectra. This probe dispersion has absolutely no effect on the results of either fits or simulations of kinetics since data at each wavelength are analyzed individually and with independent zerotimes (i.e., in the same manner as with single-wavelength detection). The instrument response as measured by the risetime of the bleaching in the long-wavelength band of P is complete by ~200 fs. (Essentially the same result is depicted in the 695-nm data shown in the insets to Figure 4). Analysis of these data as the integral of a Gaussian returns a width that is the same as the ~150-fs autocorrelation width of the laser pulse (corresponding to a pulse width of ~100 fs). The instrument function was incorporated in the simulations of Figure 4 by convoluting it with the appropriate function for sequential kinetic steps in the models evaluated. It is important to note that the instrument risetime is much shorter than the time scale of the critical data evaluated in this work; it does not affect either the measured or simulated ΔAs at times greater than ~200 fs.

Our standard sample arrangement was used in which 3.5 mL of *Rhodobacter sphaeroides* R26 RCs was flowed through

† This work was supported by the National Science Foundation, Grant DMB-8903924.

0006-2960/91/0430-609$02.50/0

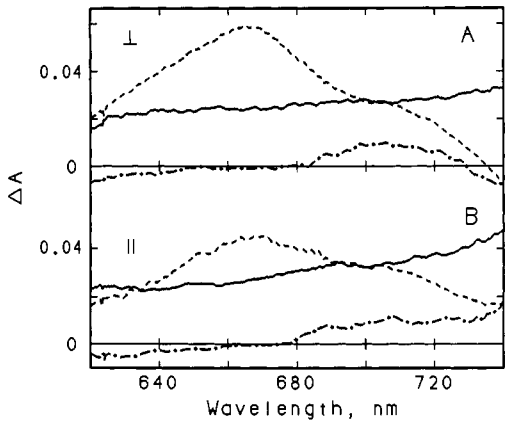

FIGURE 1: Transient absorption spectra taken 0.5 ps (—), 15 ps (---), and 2 ns (-·-) after excitation of *Rb. sphaeroides* RCs using perpendicular (part A) and parallel (part B) relative polarizations of the 870-nm pump and white-light probe flashes. Approximately 20% of the RCs in the sample were excited. The delay times are with respect to zerotime at ~690 nm; see Experimental Procedures for further details.

a 2-mm path-length cell while being maintained at 10 °C via connection to a reservoir held in an ice bath. This flow system has the advantages of keeping the RCs cool and of exciting an individual RC a minimal number of times integrated over the course of an experiment. (Typically, an RC will turn over only 10–30 times depending on the length of the experiment, the excitation conditions, and sample concentration.) The RC samples used were ~40 μM, giving the same optical density of 1 at 865 nm as used by Holzapfel et al. (1990), where ~80 μM RCs were studied in a 1-mm cell.

Results

Before kinetic data were acquired, a series of spectra of $P^+BPh_L^-$ at delay times from 15 to 20 ps were acquired for both parallel and perpendicular relative polarizations of the pump and probe pulses as a function of 870-nm excitation energy. [We will refer to the data acquired with the two relative pump/probe polarizations as simply parallel (or ||) data and perpendicular (or ⊥) data.] These control measurements verified that the magnitude of the absorption changes varied linearly with excitation energy and that the polarization of the 665-nm BPh_L anion transition with respect to the 870-nm transition of P did not vary with excitation energy, even to energies higher than typically employed. Under conditions where 2% to as high as 30% of the RCs were excited, the 665-nm BPh_L anion band polarization was found to be 66° ± 2°. This is the same value that we have reported previously and is the angle expected on the basis of the calculated direction of this transition in the tetrapyrrole macrocycle (Petke et al., 1981) and the RC structure (Michel et al., 1986; Yeates et al., 1988) as discussed elsewhere (Kirmaier et al., 1989). An angle of 68° ± 2° was measured by Holzapfel et al. (1990), which confirms our previous result. More importantly, the agreement upon this value and the similarities in the experimental conditions establish a foundation for further direct comparison of the data of Holzapfel et al. (1989, 1990) with those reported here.

The absorption changes between 620 and 740 nm were measured at 100 delay times spanning a few picoseconds before excitation to 2 ns after excitation for both parallel and perpendicular polarizations. Parts A and B of Figure 1 show ⊥ and || spectra, respectively, which can be used as guides for the absorption changes which occur upon the transformation of P* (—) to $P^+BPh_L^-$ (---) to $P^+Q_A^-$ (-·-). We focus first

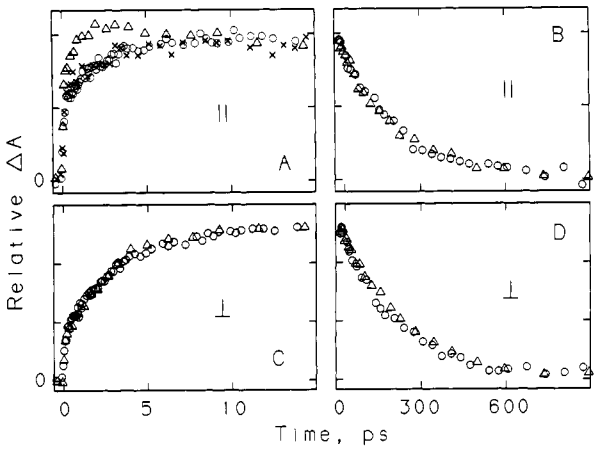

FIGURE 2: Kinetic data at 665 nm taken under the same conditions as in Figure 1 (circles) and for ~5% excitation of the sample (×'s in part A). The triangles are the 665-nm data digitized and replotted from Holzapfel et al. (1990). Parts A and C compare the parallel and perpendicular data, respectively, on the ≤15-ps time scale of BPh_L reduction. Parts B and D compare the parallel and perpendicular data, respectively, at times of ≥15 ps for electron transfer from BPh_L^- to Q_A. [Our data extend to 2 ns but are truncated at 900 ps for comparison with the data from Holzapfel et al. (1990).] The data from the two studies were normalized on the basis of the ΔA measured between 15 and 25 ps.

on the data at 665 nm, the peak of the BPh_L anion band, since this is the wavelength where key || and ⊥ kinetic data were reported by Holzapfel et al. (1989, 1990). Figure 2 (circles) shows the time course of the absorption changes at 665 nm accompanying reduction of BPh_L (parts A and C) and electron transfer from BPh_L^- to Q_A (parts B and D) for both parallel (parts A and B) and perpendicular (parts C and D) polarizations. For comparison purposes, the data of Holzapfel et al. (1990) are plotted as the triangles in Figure 2. The data sets from the two studies have been normalized on the basis of the absorption changes measured solely in the window between 15 and 25 ps; there is agreement between the two studies on the polarization of the BPh_L anion band determined from the || and ⊥ data in this window (see above), providing this unambiguous reference point for comparison of the data.

It can be seen immediately that the data in these two studies have about the same signal-to-noise ratio, and in three of the four panels the data are essentially indistinguishable. (The latter point also attests to the validity of the normalization method.) Focusing first on $P^+BPh_L^- \rightarrow P^+Q_A^-$ electron transfer, our data give time constants for this process of 206 ± 9 ps (|| data) and 215 ± 12 ps (⊥ data). This ~200-ps time constant is the same as has been measured previously by many workers and as the 220 ps Holzapfel et al. (1990) used in modeling their data. The ⊥ data for the early time course of the absorption changes in the two studies are also in good agreement (Figure 2C). However, beginning immediately after the initial instrument rise and extending to ~5 ps, there is a clear divergence between the data sets for the || absorption changes (Figure 2A). The additional rise in transient absorption (with a peak near 2–3 ps) and subsequent decay to lower value at longer times (e.g., 15 ps) in the triangle data have been interpreted as the buildup and decay of the short-lived (τ ~0.9 ps) intermediate $P^+BChl_L^-$ (Holzapfel et al., 1990). In contrast our || data are similar to our ⊥ data in that both show a smooth growth of transient absorption between 0.2 and 15 ps. We also acquired data at the level of ~5% excitation, which are given for the || experiment by the ×'s in Figure 2A (normalized as above). At this level of excitation our signal-to-noise ratio is reduced, but the con-

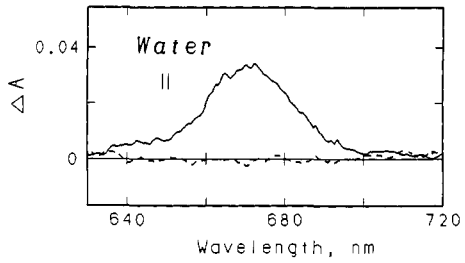

FIGURE 3: Inverse Raman band of water observed during temporal overlap of pump and probe flashes polarized parallel to one another (solid spectrum). A 2-mm path-length cell of water and ~10-μJ 870-nm flashes focused to <1 mm were used. The magnitude of this feature depends on the experimental conditions and can be much smaller than that shown in this example; see text. The dashed spectrum was acquired at 0.5 ps.

clusion that our parallel data differ significantly from that of Holzapfel et al. in the 0.2- to ~5-ps time window remains the same.

Discussion

Our recent results (Kirmaier & Holten, 1990) and those of Holzapfel et al. (1989, 1990) indicate that the early time course of the absorption changes in the near-infrared (750–820 nm) are not uniformly described by a simple single-exponential function. The question is therefore not so much one of do kinetic complexities exist but rather to what can they be ascribed. We have suggested that the complexity reflects at least in part a distribution of RCs and the associated distributed kinetics with which the question of formation and decay of $P^+BChl_L^-$ is convoluted. Holzapfel et al. take the simpler view of a homogeneous system wherein the observed kinetic complexity indicates that $BChl_L$ is an electron carrier between P* and BPh_L.

Since the anion region is rather simple in its spectral composition, it is relatively straightforward to do rational modeling of the 620–740-nm absorption changes under different kinetic schemes. Before turning to this, the discrepancy between the ∥ data in Figure 2A warrants discussion, although at the outset we can say there seems no satisfactory explanation. For example, a buildup of oxidized RCs can be discounted as a problem since attempts to excite a sample of RCs fully oxidized with $K_3Fe(CN)_6$ were unsuccessful in generating any transients. (This is not surprising since oxidized RCs have essentially no absorption at the 870-nm excitation wavelength.)

Another possibility is short-lived Raman features. For a given excitation wavelength, stimulated Raman manifests as probe gain (i.e., it appears as a bleaching) on the Stokes side of the excitation wavelength and the corresponding inverse Raman band as an absorption (probe depletion) to the blue of the excitation wavelength (Alfano & Shapiro, 1971). Such features are seen only during temporal overlap of the pump and probe pulses, their magnitude depends on the energy of the pump pulse and pump/probe phase matching conditions, and in our experience they are almost always associated with the solvent. For example, toluene gives sharp stimulated Raman and inverse Raman features at 710 and 493 nm, respectively, when 582-nm excitation is used. Water gives a broad inverse Raman absorption ~3400 cm^{-1} to the blue of 870-nm excitation (i.e., near 670 nm) as shown in Figure 3. Since this is a coherent effect, the feature is observed only with parallel pump/probe polarization and is not seen in a ⊥ experiment (data not shown). Under the excitation conditions we used for the RC experiments reported here, water (buffer solutions) did not give a detectable inverse Raman band. This process should not have given rise to the extra transient absorption observed by Holzapfel et al. (1989, 1990) unless there were wings on the excitation pulse or a reflection of the pulse in the system giving rise to a delayed effect. Thus, at this point the discrepancy seen in the data of Figure 2A remains unexplained. However, the inverse Raman absorption described here will be relevant to future picosecond studies in the anion region attempting to resolve transients such as $P^+BChl_L^-$ or processes such as relaxations of P* if their detection approaches being instrument-limited.

Models for Initial Charge Separation. As mentioned above, the anion region provides a relatively clean spectral window where only P*, BPh_L^-, and $BChl_L^-$ (if it forms) have substantial absorption. There is no significant ground-state absorption to provide complicating bleachings and electrochromic shifts as exist in abundance in the Q_Y region. $P^+Q_A^-$ also is relatively silent in this region, particularly near 665 nm (–·– spectra, Figure 1), as is well-known from simple static P^+ difference spectra (Parson & Cogdell, 1975). On the basis of in vitro studies, the $BChl_L$ anion band should be broad like that of BPh_L^- and have roughly the same (or a slightly smaller) peak extinction coefficient (ϵ) as the BPh_L^- band but with a somewhat red-shifted position (Fajer et al., 1975). The exact position of the $BChl_L^-$ band is of course unknown; however, the recent observation of a BChl anion band at 690 nm with approximately the same peak ϵ as BPh_L^- in a genetically engineered *Rb. sphaeroides* RC is relevant and consistent with the expectations from in vitro spectroscopy (Kirmaier et al., 1991). Calculations suggest that the anion transition of both BChl and BPh should lie roughly along the Q_Y (N_1–N_3) direction of the macrocycle (Petke et al., 1981). This together with the RC X-ray data (Michel et al., 1986; Yeates et al., 1988) suggests that the polarization of the $BChl_L$ anion band with respect to the 870-nm transition of P should be roughly 30°; the predicted and measured value for BPh_L^- is ~65°. Given these spectral properties, it is a simple matter to model the ∥ and ⊥ kinetic data at any wavelength in the anion region under various kinetic schemes. It is important to note that although the formation and decay of $P^+BChl_L^-$ would be most readily seen in the ∥ data, it must be manifest in both ∥ and ⊥ data except at wavelengths where $P^+BChl_L^-$ has exactly the same ϵ as $P^+BPh_L^-$ (again taking dichroism into account).

Holzapfel et al. (1989, 1990) have modeled their data in terms of the sequential steps $P^* \rightarrow P^+BChl_L^- \rightarrow P^+BPh_L^- \rightarrow P^+Q_A^-$, using P*, $P^+BChl_L^-$, and $P^+BPh_L^-$ lifetimes of 3.5, 0.9, and 220 ps, respectively. They show that, in order to account for their absorption changes between 0.2 and 5 ps in Figure 2A (triangles), the $BChl_L^-$ intermediate contributes in a ∥ experiment with $\epsilon_\parallel$ at 665 nm ~3 times larger than that of BPh_L^-. A problem with this result is that it requires the inherent ϵ (that in the absence of photodichroism) of the $BChl_L$ anion to be ~1.5 times larger than the BPh_L anion ϵ at 665 nm, *the peak* of the BPh_L^- band. Furthermore, if the $BChl_L$ anion band does not peak at 665 nm but at longer wavelengths as expected (and as Holzapfel et al. indicate to be the case), then $BChl_L^-$ would have a peak ϵ even larger still compared to that of BPh_L^-. In either case, the $BChl_L^-$ spectrum would not be in keeping with the in vitro spectral properties described above. While one can always invoke electrostatic effects of P^+ or the protein to circumvent this problem, the BPh and BChl anions observed to date in comparative studies of a variety of wild-type and modified RCs have all had the same peak ϵ's (to within ~10%) and have shown good correlation with the basic in vitro spectroscopic properties of the chromophores [see, e.g., Kirmaier et al. (1991)]. Another possibility to allow for the ∥ triangle data would be for the po-

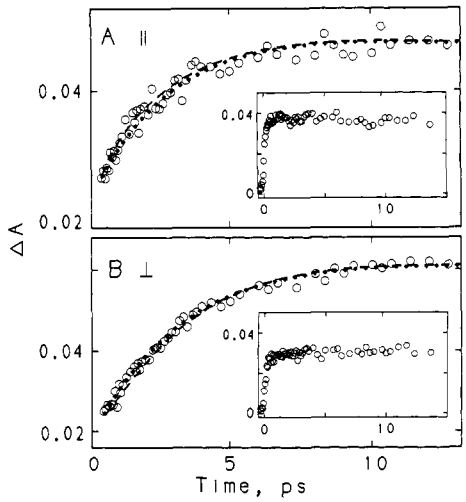

FIGURE 4: Simulations of the time course of the absorption changes at 665 nm under the $P^* \rightarrow P^+BPh_L^- \rightarrow P^+Q_A^-$ model (···) and the $P^* \rightarrow P^+BChl_L^- \rightarrow P^+BPh_L^- \rightarrow P^+Q_A^-$ model (---). The lifetimes and relative extinction coefficients of the species are given in the text. Simulations for parallel and perpendicular absorption changes are given in parts A and B, respectively, in comparison to our data (circles). (To make maximum use of the vertical scale in this display, data and simulations through the ~0.2-ps instrument risetime are not shown.) The absorption changes at 695 nm are shown in the insets.

larization of the $BChl_L^-$ transition to be very small (e.g., 10°). However, this will have negative consequences on the ability to simultaneously account for the ⊥ data. The point remains that, in addition to the key parallel data of Holzapfel et al. not being reproduced here, the implications of those data on the basic spectroscopic properties of the molecules merit some consideration.

Even though our 665-nm data are different, Figure 4 shows that they are easily modeled under either a one- or two-step mechanism for initial charge separation with very reasonable parameters. For the former model ($P^* \rightarrow P^+BPh_L^- \rightarrow P^+Q_A^-$), the lifetimes of P* and $P^+BPh_L^-$ were taken to be 3 and 200 ps, respectively, and $\epsilon_\perp/\epsilon_\parallel = 1.33$ for BPh_L^- was used. (This ratio gives a 65° polarization angle for the BPh_L anion transition.) The simulated kinetics are given by the dotted lines through our data in Figure 4. Keeping all these parameters fixed, state $P^+BChl_L^-$ was added (to model $P^* \rightarrow P^+BChl_L^- \rightarrow P^+BPh_L^- \rightarrow P^+Q_A^-$) with a lifetime of 0.6 ps and with $\epsilon_\parallel(BChl_L^-)/\epsilon_\parallel(BPh_L^-) = 1.33$ and $\epsilon_\perp(BChl_L^-)/\epsilon_\perp(BPh_L^-) = 0.5$. (These $\epsilon_\parallel$ and $\epsilon_\perp$ parameters are appropriate for an ~30° polarization angle for the $BChl_L^-$ transition and for an inherent ϵ for $BChl_L^-$ ~25% smaller than that of BPh_L^- at 665 nm.) The simulated kinetics using these parameters are given by the dashed lines in Figure 4. The parameters used in these two models should not be taken as necessarily giving the best or the only good simulations of the data; some variation of any of the parameters is found to give good simulations. It is worth noting, however, that if the lifetime of $P^+BChl_L^-$ is made longer than about 0.6 ps, the two-step simulation begins to show significant deviations from our data, which would have to be compensated for by lowering the $BChl_L^-$ ϵ and/or by raising the polarization angle of the transition. Again, the fundamental implications of such adjustments would need to be kept in mind. The main point to be made from Figure 4 is that with very reasonable parameters the simulations of the one- and two-step models account about equally well for the early time course of our 665-nm data.

Having the $P^+BChl_L^-$ contribution at 665 nm somewhat smaller than that of $P^+BPh_L^-$ in our simulations will accommodate the peak of the $BChl_L$ anion being at 665 nm (but smaller than that of BPh_L^-) or the $BChl_L^-$ peak being elsewhere (e.g., in the vicinity of 690 nm) as suggested above. It is instructive to examine the kinetics near 690 nm since, from modeling their data, Holzapfel et al. (1990) derived the peak in the spectrum they assign to the 0.9-ps component (i.e., to $P^+BChl_L^-$) to be near this wavelength. Their kinetic data near 690 nm were not shown, however. Our kinetic data at 695 nm are shown in the insets to Figure 4, and it can be seen that, far from revealing the appearance of a short-lived intermediate (particularly in the || data), the data for *both* polarizations show essentially isosbestic behavior for many picoseconds after the 100-fs flash.

The time course of the absorption changes throughout 620–740 nm have been examined in intervals of ≤5 nm, and the data shown here at 665 and 695 nm represent the extremes of the behavior observed. At 665 nm one sees the largest spectral change with time as $P^+BPh_L^-$ forms. To shorter and longer wavelengths the change in ΔA with time becomes smaller, with isosbestic behavior observed throughout the P* lifetime at wavelengths indicated in Figure 1 where the P* and $P^+BPh_L^-$ spectra (solid and dashed, respectively) are the same. Specifically, the || and ⊥ data show isosbestic or nearly isosbestic behavior between ~690 and ~710 nm. At no wavelength is unambiguous evidence found for a short-lived intermediate. Thus, it seems difficult to simultaneously model our || and ⊥ data throughout the 620–740-nm region under the two-step mechanism unless (i) the $BChl_L$ anion deviates significantly from the basic spectral parameters expected for it and/or (ii) $P^+BChl_L^-$ has a lifetime shorter than ~0.5 ps. These possibilities cannot be rejected outright, of course. Thus, while our anion region data as a whole are more easily reconciled with an alternative mechanism for initial charge separation such as superexchange, as are the results of a number of other recent experimental investigations (Breton et al., 1988; Kirmaier et al., 1990; Lockhart et al., 1988, 1990; Wasielewski & Tiede, 1986; Woodbury et al., 1985), the two-step mechanism in some form is not disproven.

ACKNOWLEDGMENTS

We thank Drs. D. Bocian, S. Boxer, W. Parson, J. Rodriguez, and N. Woodbury for helpful comments.

REFERENCES

Alfano, R. R., & Shapiro, S. L. (1971) *Chem. Phys. Lett. 8*, 631–633.

Bixon, M., Jortner, J., Michel-Beyerle, M. E., & Ogrodnik, A. (1989) *Biochim. Biophys. Acta 977*, 273–286.

Breton, J., Martin, J.-L., Fleming, G. R., & Lambry, J.-C. (1988) *Biochemistry 27*, 8276–8284.

Fajer, J., Brune, D. C., Davis, M. S., Forman, A., & Spaulding, L. D. (1975) *Proc. Natl. Acad. Sci. U.S.A. 72*, 4956–4960.

Friesner, R. A., & Won, Y. (1989) *Biochim. Biophys. Acta 977*, 99–122.

Holzapfel, W., Finkele, U., Kaiser, W., Oesterhelt, D., Scheer, H., Stilz, H. U., & Zinth, W. (1989) *Chem. Phys. Lett. 160*, 1–7.

Holzapfel, W., Finkele, U., Kaiser, W., Oesterhelt, D., Scheer, H., Stilz, H. U., & Zinth, W. (1990) *Proc. Natl. Acad. Sci. U.S.A. 87*, 5168–5172.

Hu, Y., & Mukamel, S. (1989) *Chem. Phys. Lett. 160*, 410–416.

Kirmaier, C., & Holten, D. (1990) *Proc. Natl. Acad. Sci. U.S.A 87*, 3552–3556.

Kirmaier, C., Holten, D., & Parson, W. W. (1983) *Biochim. Biophys. Acta 725*, 190–202.

Kirmaier, C., Holten, D., & Parson, W. W. (1985) *Biochim. Biophys. Acta 810*, 33-48, 49-61.
Kirmaier, C., Bylina, E. J., Youvan, D. C., & Holten, D. (1989) *Chem. Phys. Lett. 159*, 251-257.
Kirmaier, C., Gaul, D., DeBey, R., Holten, D., & Schenck, C. (1991) *Science* (in press).
Kitzing, E. V., & Kuhn, H. (1990) *J. Phys. Chem. 94*, 1699-1702.
Lockhart, D. J., Goldstein, R. F., & Boxer, S. G. (1988) *J. Phys. Chem. 89*, 1408-1415.
Lockhart, D. J., Kirmaier, C., Holten, D., & Boxer, S. G. (1990) *J. Phys. Chem. 94*, 6987-6995.
Marcus, R. A. (1988) *Chem. Phys. Lett. 146*, 13-22.
Michel, H., Epp, O., & Deisenhofer, J. (1986) *EMBO J. 5*, 2445-2451.
Parson, W. W., & Cogdell, R. J. (1975) *Biochim. Biophys. Acta 416*, 105-149.
Petke, J. D., Maggiora, G. M., Shipman, L. L., & Christoffersen, R. E. (1981) *Photochem. Photobiol. 33*, 663-671.
Scherer, P. O. J., & Fischer, S. F. (1989) *Chem. Phys. 131*, 115-127.
Warshel, A., Creighton, S., & Parson, W. W. (1988) *J. Phys. Chem. 92*, 2696-2701.
Wasielewski, M. R., & Tiede, D. M. (1986) *FEBS Lett. 204*, 368-372.
Woodbury, N. W., Becker, M., Middendorf, D., & Parson, W. W. (1985) *Biochemistry 24*, 7516-7521.
Yeates, T. O., Komiya, H., Chirino, A., Rees, D. C., Allen, J. P., & Feher, G. (1988) *Proc. Natl. Acad. Sci. U.S.A. 85*, 7993-7997.

Articles

Catalysis of the Oxidative Folding of Ribonuclease A by Protein Disulfide Isomerase: Dependence of the Rate on the Composition of the Redox Buffer†

Michelle M. Lyles and Hiram F. Gilbert*
Verna and Marrs McLean Department of Biochemistry, Baylor College of Medicine, Houston, Texas 77030
Received May 4, 1990; Revised Manuscript Received September 26, 1990

ABSTRACT: The velocity of the oxidative renaturation of reduced ribonuclease A catalyzed by protein disulfide isomerase (PDI) is strongly dependent on the composition of a glutathione/glutathione disulfide redox buffer. As with the uncatalyzed, glutathione-mediated oxidative folding of ribonuclease, the steady-state velocity of the PDI-catalyzed reaction displays a distinct optimum with respect to both the glutathione (GSH) and glutathione disulfide (GSSG) concentrations. Optimum activity is observed at [GSH] = 1.0 mM and [GSSG] = 0.2 mM. The apparent k_{cat} at saturating RNase concentration is 0.46 ± 0.05 μmol of RNase renatured min^{-1} (μmol of PDI)$^{-1}$ compared to the apparent first-order rate constant for the uncatalyzed reaction of 0.02 ± 0.01 min^{-1}. Changes in GSH and GSSG concentration have a similar effect on the rate of both the PDI-catalyzed and uncatalyzed reactions except under the more oxidizing conditions employed, where the catalytic effectiveness of PDI is diminished. The ratio of the velocity of the catalyzed reaction to that of the uncatalyzed reaction increases as the quantity $[GSH]^2/[GSSG]$ increases and approaches a constant, limiting value at $[GSH]^2/[GSSG]$ greater than 1 mM, suggesting that a reduced, dithiol form of PDI is required for optimum activity. As long as the glutathione redox buffer is sufficiently reducing to maintain PDI in an active form ($[GSH]^2/[GSSG] > 1$ mM), the rate acceleration provided by PDI is reasonably constant, although the actual rate may vary by more than an order of magnitude. PDI exhibits half of the maximum rate acceleration at a $[GSH]^2/[GSSG]$ of 0.06 ± 0.01 mM.

Protein disulfide isomerase (PDI)[1] was initially isolated by Anfinsen and his colleagues (Goldberger et al., 1963) on the basis of the ability of the protein to catalyze the oxygen or glutathione disulfide dependent renaturation of RNase A from the reduced enzyme (Epstein et al., 1963). PDI (M_r 57 800) is localized primarily in the endoplasmic reticulum as a luminal, peripheral membrane protein (Lambert & Freedman, 1983). The enzyme exhibits broad specificity and, in addition to catalyzing disulfide bond formation and rearrangement in proteins, accelerates thiol/disulfide exchange reactions involving numerous protein and nonprotein substrates (Hillson et al., 1984; Morin & Dixon, 1985; Varandani et al., 1975). This lack of specificity is uncharacteristic of conventional enzymes but is in keeping with the necessity for catalyzing the formation, rearrangement, and reduction of disulfide bonds between cysteine residues in a number of sequence contexts.

Surprisingly, PDI has also been shown to function as the β-subunit of prolyl hydroxylase (Pihlajaniemi et al., 1987), one of the subunits of a triglyceride transfer complex of the endoplasmic reticulum (Wetterau et al., 1990), a thyroid hormone binding protein (Yamauchi et al., 1987), and as a component of the glycosylation apparatus of the ER–Golgi complex (Geetha-Habib et al., 1988). This has naturally led to disagreement about the in vivo role of this protein. Homology is observed between PDI and thioredoxin, suggesting that PDI contains two thioredoxin-like domains, each with a dithiol/disulfide pair (Edman et al., 1985; Freedman et al.,

† This work was supported by NIH Grant GM-40379.

[1] Abbreviations: PDI, protein disulfide isomerase; RNase A, bovine pancreatic ribonuclease A; BPTI, bovine pancreatic trypsin inhibitor; GSH, glutathione; GSSG, glutathione disulfide; DTT, dithiothreitol.

0006-2960/91/0430-613$02.50/0